McCoy TJ, Keil K, Clayton RN, Mayeda TK, Bogard DD, Garrison DH, Huss GR, Hutcheon ID, Wieler R (1996) A petrologic, chemical and isotopic study of monument draw and comparison with other acapulcoites: evidence for formation by incipient partial melting. Geochim Cosmochim Acta 60:2681–2708
McKay DS, Gibson EK, Thomas-Keprta VH, Romanek CS, Clement SJ, Chillier XDF, Maechling CR, Zare RN (1996) Search for past life on Mars: possible relic biogenic activity in martian meteorite ALH84001. Science 273:924–930
McSween HY Jr (2002) The rocks of Mars, from far and near. Meteorit Planet Sci 37:7–25
McSween HY Jr, Treiman AH (1998) Martian meteorites. In Planetary Materials (J.J. Papike ed.) Rev Mineral 36:6-1–6-53
Mittlefehldt DW (1994) ALH84001, a cumulate orthopyroxenite member of the martian meteorite clan. Meteoritics 29:214–221
Mittlefehldt DW, Lindstrom MM (1990) Geochemistry and genesis of the Angrites. Geochim Cosmochim Acta 54:3209–3218
Mittlefehldt DW, McCoy TJ, Goodrich CA, Kracher A (1998) Non-chondritic meteorites from asteroidal bodies in planetary materials (J.J. Papike, ed.) Rev Mineral 36:4.1–4.495
Nagahara H (1992) Yamato-8002: partial melting residue on the “unique” chondrite parent body. Proc NIPR Symp Antarct Meteorit 5:191–223
Nyquist LE, Bogard DD, Shih C-Y, Greshake A, Stöffler D, Eugster O (2001) Ages and geologic histories of martian meteorites. Space Sci Rev 96:105–164
Palme H, Jones A (2003) Solar abundances of the elements. In: Davis AM (ed) Treatise on geochemistry 1, meteorites, comets, and planets. Elsevier-Pergamon, Oxford, pp 41–61
Paniello R, Day JMD, Moynier F (2012) Zn isotopic evidence for the origin of the moon. Nature 490:376–379
Papike JJ, Ryder G, Shearer CK (1998) Lunar samples. In planetary materials (J.J. Papike. Ed.) Rev Mineral 36:5.1–5.234
Rubin AE, Grossman JN (2014) Meteorite and meteoroid: a new comprehensive definition. Meteorit Planet Sci 45:114–122
Savage PS, Moynier F (2013) Silicon isotopic variation in enstatite meteorites: clues to their origin and earth-forming material. Earth Planet Sci Lett 361:487–496
Scott ERD (1972) Chemical fractionation in iron meteorites and its interpretation. Geochim. Cosmochim. Acta 36:1205–1236
Scott ERD, Wasson JT (1975) Classification and properties of iron meteorites. Rev Geophys Space Phys 13:527–546
Scott ERD, Haack H, Love SG (2001) Formation of mesosiderites by fragmentation and reaccretion of a large differentiated asteroid. Meteorit Planet Sci 36:869–881
Sears DWG, Kallemeyn GW, Wasson JT (1982) The compositional classification of chondrites: II The enstatite chondrite groups. Geochim Cosmochim Acta 46:597–608
Warren PH (2011) Stable-isotopic anomalies and the accretionary assemblage of the earth and Mars: a subordinate role for carbonaceous chondrites. Earth Planet Sci Lett 311:93–100
Wasson JT, Kallemeyn GW (1988) Composition of chondrites. Philos Trans R Soc Lond A325:535–544
Watters TR, Prinz M (1979) Aubrites: their origin and relationship to enstatite chondrites. Proc Lunar Planet Sci Conf 10:1073–1093
Weisberg MK, McCoy TJ, Krot AE (2006) Systematics and evaluation of meteorite classification. In: Lauretta D, McSween HY Jr (eds) Meteorites and the early solar system II. University of Arizona Press, Tucson, pp 19–52
Weisberg MK, Ebel DS, Nagashima D, Kita N, Humayun M (2015) Petrology and geochemistry of chondrules and metal in NWA 5492 and GRO 95551: a new type of metal-rich chondrite. Geochim Cosmochim Acta 167:269–285
Weiss BP, Gattacceca J, Sabine S, Rochette P, Christensen UR (2010) Paleomagnetic record of meteorites and early planetesimal differentiation. Space Sci Rev 152:341–390
Wheelock MM, Keil K, Floss C, Taylor GJ, Crozaz G (1994) REE geochemistry of oldhamite-dominated clasts from the Norton County aubrite: igneous origin of oldhamite. Geochim Cosmochim Acta 58:449–458
Yanai K (1994) Angrite Asuka-881371: preliminary examination of a unique meteorite in the Japanese collection of Antarctic meteorites. Proc NIPR Symp Antarct Meteorites 7:30–41

Mid-Ocean Ridge Basalts (MORB)

Charles H. Langmuir
Department of Earth and Planetary Sciences, Harvard University, Cambridge, MA, USA

Definition

Mid-ocean ridge basalts are the volcanic rocks erupted at the global system of ocean ridges. They are the most common volcanic rock type on Earth. They provide insights into the mantle from which they are derived by partial melting and the processes in ocean ridge volcanic systems through which they pass on their way to the surface.

Introduction

The global system of ocean ridges is a continuous line of volcanism that wraps around the globe reaching a total length of more than 60,000 km. Ridges are the sites of formation of new oceanic crust, and over time have created the entire ocean floor, with the exception of some additions through intraplate volcanism and sediments that gradually accumulate as the crust ages. The rocks created at ocean ridges are the most common rocks on Earth, covering two-thirds of the Earth’s surface, i.e., oceanic crust. Ocean ridge volcanism is about 75% of all volcanic activity on Earth (Crisp 1984), but is largely hidden from view since most of it occurs several thousand meters below sea level. The ocean ridge volcanoes erupt basaltic magmas called “ocean ridge basalt.” While not all ocean ridges are in the middle of their hosting oceans, this basalt has become known as “mid-ocean ridge basalt,” or MORB. MORB is the most common volcanic rock type in the world.

MORB began to be investigated only in the 1960s, just after the discovery of the mid-ocean ridge and the development of plate tectonics. Steady sampling over the last 50 years has gradually provided data on more than 30,000 samples that can be used to define the average composition and variability on all scales. With the advent of a global public database, PETDB (www.petdb.org) (Lehnert et al. 2000), all published location and geochemical data for these ocean ridge samples

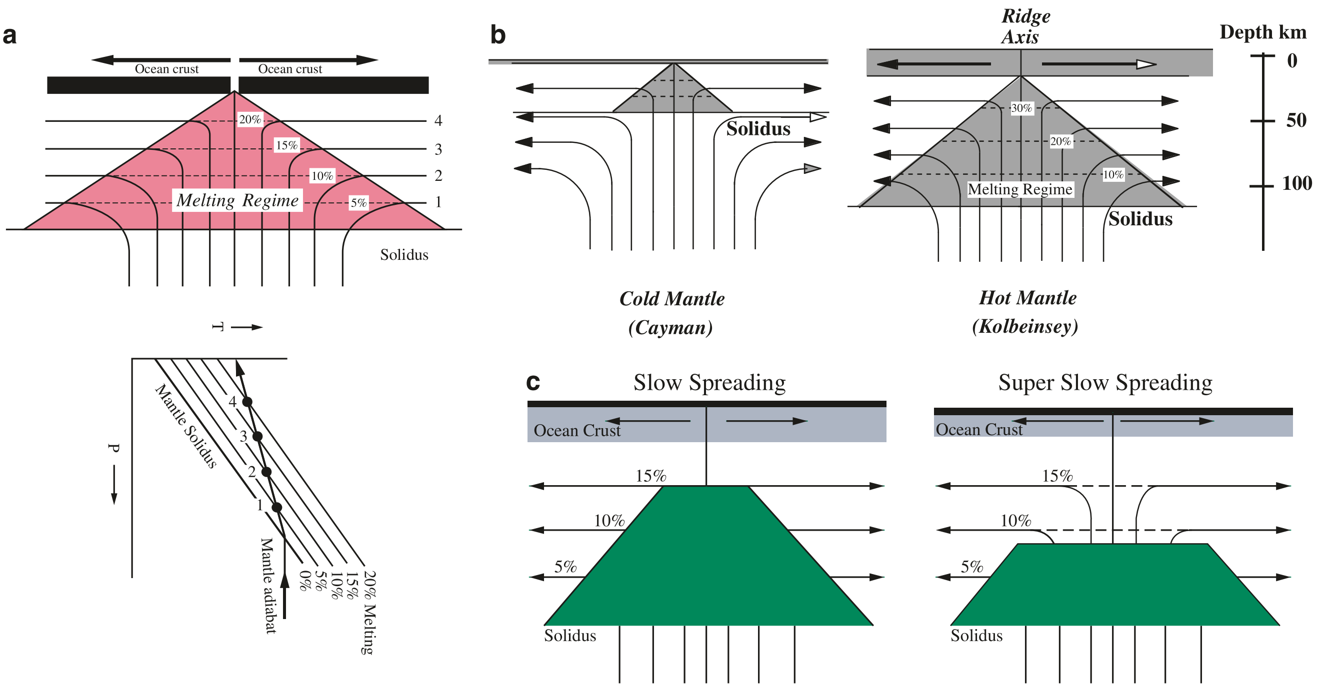

Mid-Ocean Ridge Basalts (MORB), Fig. 1 Illustration of the means by which parental magmas for MORB are generated in the mantle. A: Demonstration of how decompression of the mantle beneath the ridge leads to a melting and a "melting regime" where melt forms and is extracted to form the oceanic crust. B: Illustration of the effect of mantle temperature on the melting regime; colder mantle intersects the solidus at shallower depths, hence melts less and creates thinner crust. C: Illustration of the effect of spreading rate on the melting regime at constant temperature. As spreading rate decreases, cooling from the surface is able to penetrate more deeply into the mantle, stopping melting at greater depth

are available. Even unpublished data from US cruises are also available. There are many additional unpublished locations and data from European, Russian, Japanese, and Chinese cruises that are not in the public domain. All samples in PETDB can be readily visualized in a geographical reference frame using GEOMAPAPP (www.geomapapp.org) (Carbotte et al. 2004). The last few decades have thus revealed and defined the most abundant rock on Earth.

MORB as a Product of Pressure Release Melting

Because the ridges are constantly spreading apart, there is little impediment to the magmas reaching the surface, and for that reason, MORB are the most direct products of Earth's interior and the least modified during ascent. The mean composition of MORB then defines the composition of Earth's most extensive crustal reservoir, and is as well the best available constraint from which the composition of the upper mantle can be inferred.

MORB compositions are influenced by the primary melt that is formed by partial melting of the mantle, and the processes of chemical exchange and removal of crystals (called "differentiation") that take place during cooling before eruption. The primary melt is influenced by the temperature, pressure, and composition of the mantle. In general, MORB are generated by "pressure release melting" (Fig. 1a). The temperature at which the mantle begins to melt, called the solidus, increases substantially with pressure. Therefore, at high pressures, the mantle is solid, but as it rises beneath the ridge, the pressure decreases, and melting begins as the solidus is crossed. The amount of melting is then controlled by the depth at which the crossing of the solidus occurs, and the distance over which the mantle rises as it melts. Mantle at higher temperatures will begin melting deeper, and hence rise further, melting more than mantle that is cooler (Fig. 1b). At very slow spreading rates, surface cooling penetrates into the mantle, causing slightly lower extents of melting in these settings (Fig. 1c). The amount of melt may also be influenced by the chemical composition of the mantle.

Once the melts exit the melting regime, they may interact with the cold mantle lid overlying the melting regime, and then cool and crystallize in the crust, forming the lower oceanic crust, before the lavas are erupted on the sea floor. The erupted melts then have been influenced by multiple processes – melting of the mantle, transport of the melts through the uppermost mantle, and cooling and crystallization within the crust. Constraints on the importance and consequences of these various processes come from experiments, theory, and the compositions of MORB themselves, and how these compositions vary in different settings around the ocean ridge system.

Average MORB Compositions

Information about the chemical compositions of MORB comes from three distinct types of measurements, all of which are available through PetDB. The first are the major elements, generally referring to those oxides that are present at levels higher than about 0.05 wt.%. The major elements are conveniently measured on MORB glasses by electron microprobe, leading to a very large data set of tens of thousands of analyses. Major elements provide information about extents of cooling in the crust, as well as the composition and extent of melting of the mantle from which they are derived. Trace elements have been more difficult to determine but now are routinely measured by inductively-coupled plasma mass spectrometry, from which thousands of analyses are available. Trace elements provide more information about the variations in the composition of the mantle source that melted. The most difficult measurements are those of the radiogenic isotopes, but for the commonly measured isotopes of Sr, Nd, and Pb, there is also a substantial data set of many thousands of measurements, with progressively less data for Hf, Os, and the noble gases. The isotopic compositions are the most direct indication of the mantle source, and because their evolution is time dependent, they also provide constraints on the long-term history of the mantle sources of MORB.

The mean composition of MORB has been best determined by Gale et al. (2013), who used all the available data from PETDB and added several thousand additional analyses. MORB volcanism occurs along long cracks in the ocean crust that are periodically offset by transform faults or other smaller offsets. These offsets demark the boundaries between ridge segments. There are about 750 ridge segments along the entire ocean ridge. To avoid the problem of uneven sampling along the ridge system, Gale et al. first constructed averages for each ridge segment, and then ridge segment averages were averaged. Earlier efforts defining mean compositions, based on simple averages of smaller numbers of samples (Sun and McDonough 1989; Hofmann 1988; Arevalo and McDonough 2010), nonetheless came up with rather similar values, suggesting the mean composition is now well determined (Table 1).

A distinctive type of ocean ridge basalt is erupted at spreading centers behind active convergent margins, called back-arc basins. These back-arc spreading centers erupt back-arc basin basalts (BABB) (Sinton and Fryer 1987) that are distinguished from MORB from open ocean spreading centers by their inclusion of an “arc component” in their chemical composition, which varies in composition with distance to the arc (Langmuir et al. 2006; Kelley et al. 2006). When the back-arc spreading center is close to the arc, the BABB have high K_2O and H_2O, reflecting contributions from the down-going slab.

Mid-Ocean Ridge Basalts (MORB), Table 1 The composition of ALL MORB

	n	ALL MORBMean	±(95% conf)
MgO	430	**7.58**	0.12
SiO_2	430	**50.47**	0.08
FeO	430	**10.43**	0.21
CaO	430	**11.39**	0.09
Na_2O	430	**2.79**	0.03
Al_2O_3	430	**14.70**	0.12
TiO_2	430	**1.68**	0.05
K_2O	430	**0.160**	0.014
P_2O_3	409	**0.184**	0.012
MnO	379	**0.184**	0.005
Ba	392	**29.2**	3.8
Be	139	**0.76**	0.05
Ce	410	**14.86**	1.26
Co	350	**43.0**	0.7
Cr	369	**249**	12
Cs	272	**0.034**	0.006
Cu	357	**74**	2
Dy	411	**6.08**	0.30
Er	410	**3.79**	0.17
Eu	411	**1.36**	0.05
Ga	300	**17.5**	0.2
Gd	386	**4.99**	0.23
Hf	398	**2.79**	0.15
Ho	404	**1.28**	0.05
La	412	**5.21**	0.53
Li	255	**6.5**	0.3
Lu	410	**0.53**	0.02
Mo	185	**0.46**	0.05
Nb	402	**5.24**	0.59
Nd	418	**12.03**	0.78
Ni	365	**92**	5
Pb	370	**0.57**	0.03
Pr	390	**2.24**	0.12
Rb	380	**2.88**	0.44
Sc	338	**39.8**	0.8
Sm	417	**3.82**	0.15
Sn	200	**0.92**	0.06
Sr	413	**129**	4
Ta	352	**0.34**	0.04
Tb	397	**0.90**	0.04
Th	395	**0.404**	0.081
Tl	200	**0.020**	0.001
U	374	**0.119**	0.013
V	337	**309**	13
W	209	**0.12**	0.02
Y	410	**36.8**	1.9
Yb	411	**3.63**	0.18
Zn	338	**91.3**	3.1
Zr	412	**116.9**	8.4
$^{87}Sr/^{88}Sr$	272	**0.702819**	0.000067
$^{143}Nd/^{144}Nd$	272	**0.513074**	0.000017
$^{206}Pb/^{204}Pb$	245	**18.412**	0.090

(*continued*)

Mid-Ocean Ridge Basalts (MORB), Table 1 (continued)

$^{207}Pb/^{204}Pb$	245	**15.515**	0.010
$^{208}Pb/^{204}Pb$	245	**38.100**	0.091
$^{176}Hf/^{177}Hf$	138	**0.283**	0.000
Sm/Nd	416	**0.325**	0.005
Zr/Hf	398	**40.64**	0.95
Ba/Th	376	**71.93**	8.32
Nb/U	366	**44.37**	1.99

In addition to BABB, other diverse components make up the global average, and the regional diversity of compositions reveals much about the composition and history of the mantle. Major elements, trace elements, and isotopes each provide different sets of information.

Major Elements and Mineralogy

The mineralogy of MORB is straightforward. Olivine is the first phase to crystallize, followed by plagioclase and then clinopyroxene. At much lower temperatures, Fe-Ti oxides and low Ca pyroxene can appear, although these phases virtually never appear as phenocrysts in MORB. In almost all sampled MORB olivine and plagioclase are the most abundant phenocrysts. Clinopyroxene is less common. Fe-Ti oxides occur largely in the groundmass. Removal of these phases during cooling in the crust and uppermost mantle leads to the "liquid line of descent," the path of compositions created by cooling and removal of crystals. Calculations based on experimental data can be used to model the liquid lines of descent very accurately. What is remarkable about many MORB suites is how well samples from a particular region lie along liquid lines of descent calculated from the highest temperature basalts from the same region. Examples of MORB suites and liquid lines of descent from different regions are shown in Fig. 2. The oxide MgO is used as the horizontal axis because it is a very effective proxy for the temperatures of erupted magmas. The mean erupted temperature appears to vary slightly with spreading rate for MORB far from hot spots (Rubin and Sinton 2007), with slightly lower eruptive temperatures at faster spreading ridges, probably because of shallower magma systems that are more efficiently cooled by the surface.

The simplicity of MORB major element variations on a segment scale, illustrated for two segments in Fig. 2, is surprising given the great complexity that has emerged from the study of the plutonic rocks of the lower portions of ocean ridges (see e.g., Lissenberg et al. 2013). Very complex processes are apparent in the plutonic rocks, leading many in that community to argue that the liquid lines of descent of MORB should be very complicated and difficult to unravel (Coogan and O'Hara 2015). Given the plutonic complexity, it is

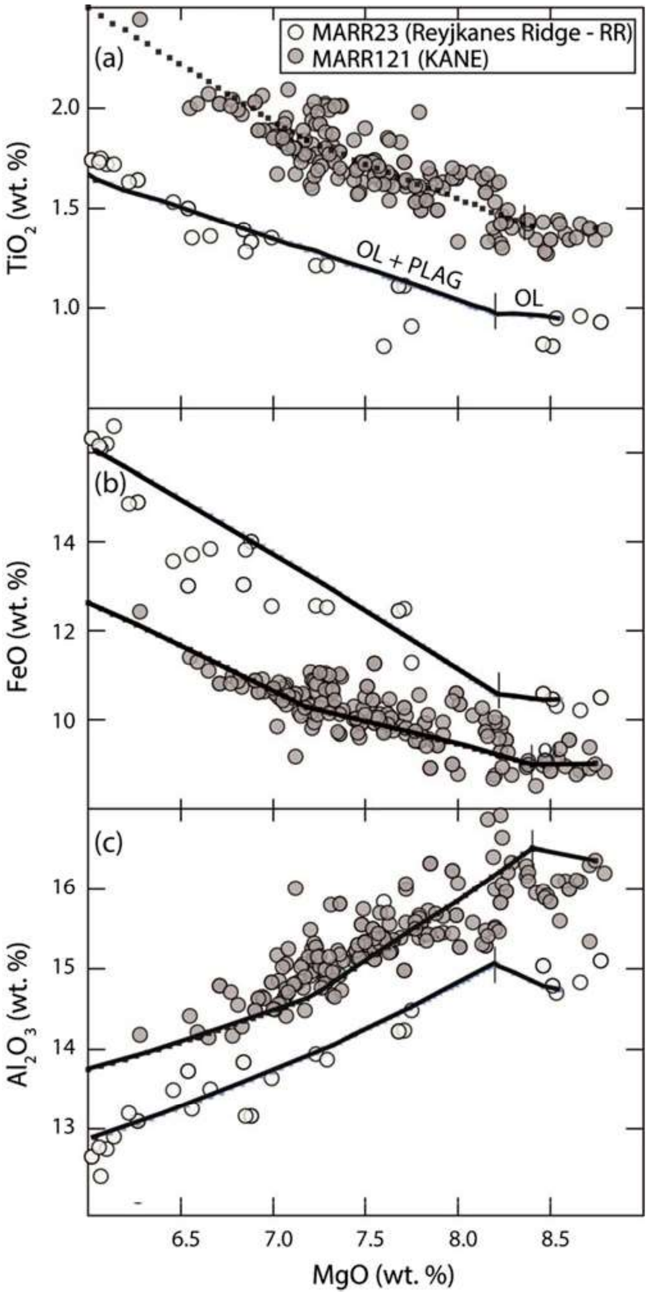

Mid-Ocean Ridge Basalts (MORB), Fig. 2 Data from a shallow (Reykjanes) and a deep (Kane) ridge segment with liquid lines of descent showing the smooth trends exhibited by lavas from individual ridge segments, and the large contrasts between mean compositions from different ridge segments. Note that the deeper ridge segment has lower Fe and Ti, and higher Al (and Na, not shown) than the shallower ridge segment (Modified from Gale et al. 2014)

remarkable how well individual MORB suites plot along simple liquid lines of descent. Whatever the origin of this fact, this observation makes it possible to back-project lower temperature MORB to the higher temperature (higher MgO) compositions that are more closely related to melts coming out of the mantle. These corrected compositions can then best be used to understand how MORB form, and what controls the variations exhibited by liquid lines of descent from different regions.

One method to correct, or normalize, compositions is to move them back along a liquid line of descent to a constant MgO content, normally 8 wt.%, which has the advantage of providing normalized compositions within the range of MORB observations (Klein and Langmuir 1987). Alternatively, compositions can be back-tracked to a composition in equilibrium with the mantle, which has an olivine composition of Fo_{90} or 90% of the MgO end-member (Stolper and Newman 1994). Gale et al. (2013) showed that the two methods produce similar results. $Na_{8.0}$ or Na_{90} refer to Na_2O contents normalized to a particular value. Normalizing in this way then allows comparisons of parental compositions around the global system of ocean ridges. These comparisons then show the systematics of MORB major element compositions, and allow a demonstration of how these systematics relate to tectonic variables such as spreading rate, proximity to hot spots, and the overall depth of the ridge axis.

Figure 3a, b shows the relationships among MORB major elements for individual ridge segments normalized to Fo_{90}, for ridge segments that have more than three samples available (Gale et al. 2014). The data are systematic and show clear relationships. Fe_{90} is negatively correlated with Si_{90}, Al_{90}, and Na_{90}, while Na_{90} and Al_{90} are positively correlated. The slowest spreading ridges, with spreading rates less than 20 mm/year, indicated by the open symbols in Fig. 3a, b, are slightly offset from the data from faster spreading ridges. There are also correlations between these chemical parameters and the depth of the segment from which the samples were recovered. Samples from shallow ridges have lower

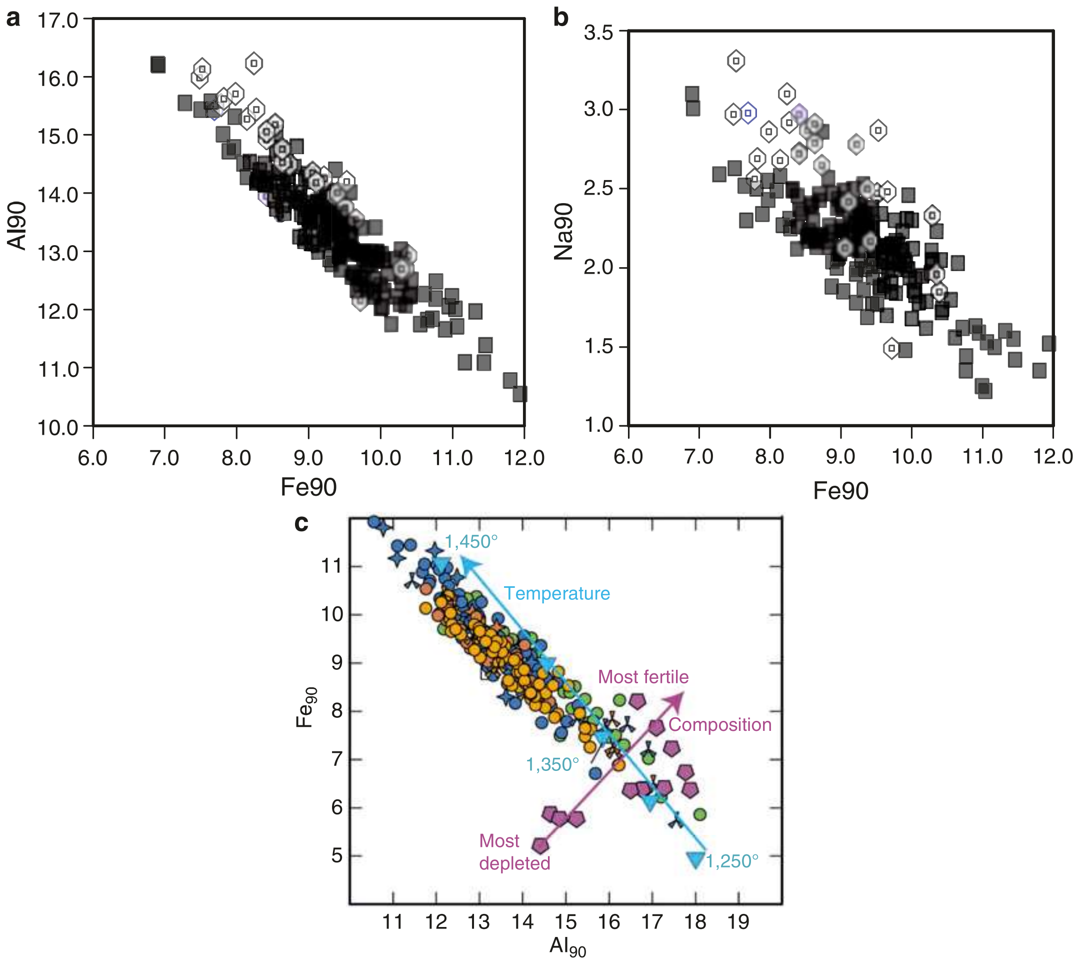

Mid-Ocean Ridge Basalts (MORB), Fig. 3 Variation of segment average major element compositions corrected to a composition in equilibrium with mantle olivine. A,B, Data for all segments except back-arc basins and hot spot centers with Th90 > 0.5. Super-slow spreading ridge segments are indicated by the open symbol. They are offset to higher Na90 and Al90 owing to a thick lithospheric lid at super-slow spreading rates. C,D Comparison of the data to trends for variable mantle temperature and variable mantle composition. *Pentagons* are experiments on mantle of different compositions. *Arrows* are calculated variations for temperature and composition. Note the principal component of the variation is well explained by mantle temperature, and not by mantle composition (Segment averages are from Gale et al. 2014)

$Na_{8.0}$, $Al_{8.0}$, and $Si_{8.0}$, and higher $Fe_{8.0}$ than samples from the deepest ridges. This contrast is also apparent by examining the liquid lines of descent in Fig. 2.

Klein and Langmuir (1987) originally proposed that these systematic variations in ocean ridge compositions were primarily the result of variations in mantle temperature, an inference that had been partially suggested on the basis of abyssal peridotite data by Dick et al. (1984). The reasoning behind this model is straightforward, and illustrated in Fig. 1b. Where the mantle is hotter, it begins melting at greater depth, and melts more as the mantle upwells toward the surface. This creates a large melting region with high extents of melting at ridges that overlie hotter mantle as compared to ridges that overlie colder mantle. The larger extents of melting dilute the Na and Al contents of the melts, while the elements Si and Fe are primarily responsive to the mean pressure of melting. The deeper average melting regime where the mantle is hot leads to higher pressures of melting and hence lower Si and higher Fe contents. The ocean crust is buoyant relative to the mantle. The large and deep melting regimes where the mantle is hotter lead to greater extents of melting and hence greater thicknesses of ocean crust, which rise to higher elevations as they equilibrate gravitationally with the underlying mantle. These early inferences remain consistent with all the new observational and experimental data.

Two alternative hypotheses have been proposed to account for the variations in ridge compositions seen in Fig. 3. Shen and Forsyth (1995) proposed that the dominant control was spreading rate. A thicker lithospheric lid at slower spreading rates (see Fig. 1c) would create smaller extents of melting, and the highest values of $Na_{8.0}$ do indeed occur primarily at the slowest spreading ridges. Niu and O'Hara (2008) proposed that the dominant control was mantle composition. They suggested that deeper ridges were underlain by sources with higher Na and lower Fe contents, which would lead to a mantle of higher density. The high density of the mantle would cause the ridge to be deep, and the high Na contents of the mantle source would lead to the high Na contents observed in basalts at the slowest spreading rates.

Both these arguments have elements of truth. As is apparent in Fig. 3a, b, the slowest spreading ridges do tend to have higher Na contents. This offset occurs across the entire range of mantle temperatures, however, and is a second-order effect. There must also be a range of mantle compositions at ocean ridges. This is very apparent in the trace element and isotope compositions, which are distinctive at and near ocean islands. Model curves for the effects of mantle composition, however, shown in Fig. 3c, d, show that the compositional variations produced by such inevitable variations are orthogonal to the main trend of the data, so this must also be a second-order effect. These conclusions are reinforced by the recent seismic data that show slower seismic velocities, and hence higher mantle temperatures, beneath ocean ridges with thicker crust (Dalton et al. 2014).

Back-arc basins also occupy a large range of mantle temperatures (Klein and Langmuir 1987; Taylor and Martinez 2003; Langmuir et al. 2006; Kelley et al. 2006), encompassing almost the entire range observed at open ocean ridges. The melting mechanisms in this environment, however, must greatly differ from the open ocean ridges, because very low $Ti_{8.0}$ and $Na_{8.0}$ at back-arc basins coincide with very low Fe contents. In general, back-arc basins are derived by higher extents of melting for the same depth as other ridges, owing to the water present in their source regions that causes higher average extents of melting in those environments.

Trace Elements

Trace elements show much larger variations than the major elements – up to a factor of 100 for the most highly incompatible elements such as Ba, Rb, and Th (Fig. 4a). These large trace element variations lead to the terms "enriched" and "depleted" when referring to MORB. The boundary between "enriched" and "depleted" generally refers to rare earth element (REE) patterns that are enriched or depleted in the lighter REE relative to chondritic meteorites, which reflect the bulk Earth composition (Sun et al. 1979) Fig. 4b). The ratio $(La/Sm)_N$, where the "N" refers to normalization to chondritic meteorites, reflects this enrichment or depletion. Since there are many more measurements of major elements than REE, the major element ratio K_2O/TiO_2 is often used as a proxy for $(La/Sm)_N$. Enriched MORB (E-MORB) have $(La/Sm)_N$ >1.5, which corresponds to K_2O/TiO_2 ~ 0.2–0.25, depending on the region. E-MORB are in part associated with ridges near ocean islands, as documented extensively by Schilling and coworkers (Schilling 1975; Schilling et al. 1982), but also occur sporadically along sections of ridges far from any known islands or hot spots. D-MORB are strongly depleted in the lighter REE, and have $(La/Sm)_N$ ~0.6. The most commonly erupted MORB, N-MORB, has $(La/Sm)_N$ of ~0.8. There has also been a term for MORB in between N-MORB and E-MORB, called T-MORB (T for transitional). A boundary between N-MORB and T-MORB would occur at $(La/Sm)_N = 0.8$, or $K_2O/TiO_2 = 0.12$. In fact, there is a continuous range from highly depleted to very strongly enriched, and the boundaries between the different classes are quite arbitrary. But generally speaking, T-MORB have flat REE patterns, E-MORB have enriched patters, and N- and D- MORB have depleted patterns. The overall trace element patters from one ocean basin to another are remarkably similar – there is a progressive continuum from "enriched" to "depleted" that is widespread.

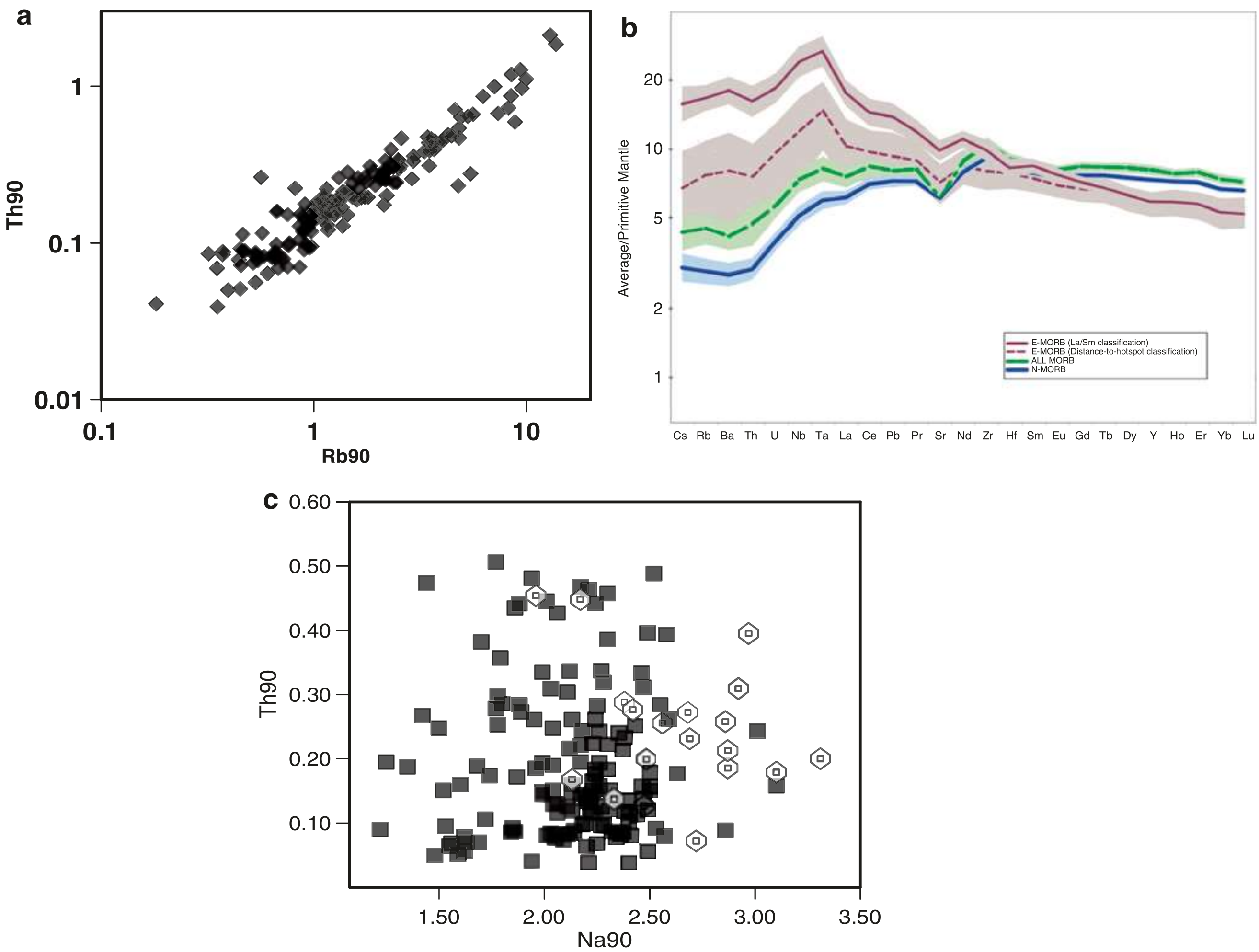

Mid-Ocean Ridge Basalts (MORB), Fig. 4 (**a**) Plot of Ba versus Th for segment averages corrected for fractionation to equilibrium with mantle olivine showing almost two orders of magnitude variations. Variations are greater than two orders of magnitude in individual samples. Note that the factor of variation far exceeds those shown for the major elements in Fig. 3 (Data from Gale et al. 2013). (**b**) Examples of normalized trace element abundances for average MORB, normal MORB far from hot spots, and enriched MORB. Normal MORB are depleted in the lighter rare earth elements (La, Ce), while enriched MORB are enriched in these and other elements. (**c**) Demonstration of the complete lack of correlation between highly incompatible elements and major elements. Segments from hot spot centers with Th90>0.5 have been excluded for clarity. They would simply extend the vertical axis to higher values

The trace element data along with the isotopes discussed below provide convincing evidence for mantle heterogeneity. The major elements suggest extents of melting vary by a factor of three – far less than would be able to account for the trace element variations. Furthermore, there is no correlation between highly incompatible elements and the major elements (Fig. 4c). In addition, enriched MORB often occur in the vicinity of ocean islands, and these regions are high temperature, leading to low abundances of elements such as Na.

Clearly, there are processes that greatly modify the highly incompatible trace element composition of the mantle without having significant effects on its major element composition. A common hypothesis for trace element-enriched MORB is the presence of recycled crust in the mantle, more enriched than the mantle itself, which melts out to produce enriched compositions (Hofmann and White 1982). A difficulty with this model is that recycled crust should also modify the major element composition of the mantle, making it difficult to explain the lack of correlation between major and trace elements. An alternative model is that the heterogeneity is created by the ubiquitous movement of low degree melts (Langmuir et al. 1992; Niu et al. 2002; Donnelly et al. 2004), which are small in mass but extremely high in trace element concentrations. Adding a percent or two of such a melt can change source abundances by orders of magnitude, while having negligible effect on the major elements. The origin of the trace element heterogeneity in MORB is far from settled.

Radiogenic Isotopes

Radiogenic isotopes show substantial variations in MORB, though much smaller in magnitude than the variations that are observed on ocean islands. The hallmark of virtually all isotopic values is that they reflect a long-term depletion of the mantle source relative to bulk Earth compositions. This depletion is consistent in general with the trace element depletion relative to chondritic meteorites. The depleted upper mantle reservoir indicated by the isotopes is widely considered to be the complement of the overall enriched compositions that characterize the continental crust.

In detail, the isotopic variations are complex (see review by White and Klein 2014). There are subtle differences between the Atlantic, Pacific, and Indian Ocean basins which are not yet clearly explained, but seem to require two distinct processes that have given rise to the diverse heterogeneity (Iwamori et al. 2010). The south Atlantic and Indian oceans are marked by variations that have been called the "Dupal anomaly" (Hart 1984), which tends to have higher values of $^{87}Sr/^{86}Sr$ at lower values of the Pb isotope ratios such as $^{206}Pb/^{204}Pb$. Within any one region, there are rough correlations between the parent/daughter ratios and the radiogenic isotopes, but this relationship is not global. This is not surprising, since trace elements can be strongly influenced by very recent processes, while the radiogenic isotopes are integrating a multibillion year history.

Outstanding Problems

The current knowledge of MORB is based almost entirely on abundant sampling along active ocean ridges where the youngest volcanic rocks are exposed. Older rocks become rapidly covered in sediment, and even when recovered they cannot be dated easily because of their alteration and very low potassium contents. It is often thought that ridges go through cycles of more and less abundant volcanism, which should be expressed in MORB compositions, and there is also the possibility of longer term variations with time. This temporal domain is virtually unexplored.

There is another large remaining conundrum, which is the relationship between the plutonic rocks that make up two-thirds of the ocean crust, and the lavas that are easily sampled at the surface. Work on the small numbers of plutonic rocks that have been recovered show a diverse set of complex processes operated on them. How this complexity can be reconciled with the very straightforward liquid lines of descent and global systematics that are evident in the erupted lavas will be an unfolding future story. How this story unfolds may also have consequences for the current interpretations of MORB compositions.

Summary

MORB are the most common rock type on Earth, and have become well characterized by five decades of study leading to tens of thousands of chemical analyses.Variations in the temperatures of eruption are largely controlled by crustal processes, which lead to liquid lines of descent at various pressures.Variations in parental magma compositions are controlled largely by mantle temperature.Hot mantle leads to higher extents of melting, thicker crust, and shallower ocean ridges.Variations in spreading rate and mantle composition are important second-order effects for the major elements and total melt production.Highly incompatible trace elements and isotopes are controlled largely by mantle heterogeneity.The relationship between the erupted volcanics and the thick plutonic sequences that make up most of the ocean crust poses puzzling problems that remain to be fully elucidated.

Cross-References

▶ Earth's Oceanic Crust
▶ Fractional Crystallization and Assimilation
▶ Geochronology and Radiogenic Isotopes
▶ Inductively Coupled Plasma Mass Spectrometry (ICP-MS)
▶ Incompatible Elements
▶ Lanthanide Rare Earths
▶ Magmatic Process Modeling
▶ Mantle Geochemistry
▶ Oceanic Island Basalts
▶ Subduction Zone Geochemistry
▶ Trace Elements

M

References

Arevalo R, McDonough WF (2010) Chemical variations and regional diversity observed in MORB. Chem Geol 271(1):70–85

Carbotte SM, Arko R, Chayes DN, Haxby W, Lehnert K, O'hara S et al (2004) New integrated data management system for Ridge 2000 and MARGINS research. EOS Trans Am Geophys Union 85(51):553–559

Coogan LA, O'Hara MJ (2015) MORB differentiation: in situ crystallization in replenished-tapped magma chambers. Geochim Cosmochim Acta 158:147–161

Crisp JA (1984) Rates of magma emplacement and volcanic output. J Volcanol Geotherm Res 20(3-4):177–211

Dalton CA, Langmuir CH, Gale A (2014) Geophysical and geochemical evidence for deep temperature variations beneath mid-ocean ridges. Science 344(6179):80–83

Dick HJB, Fisher RL, Bryan WB (1984) Mineralogical variations of the uppermost mantle along ocean ridges. Earth Planet Sci Lett 7:7–106

Donnelly KE, Goldstein SL, Langmuir CH, Spiegelman M (2004) Origin of enriched ocean ridge basalts and implications for mantle dynamics. Earth Planet Sci Lett 226:347–366

Gale A, Dalton CA, Langmuir CH, Su Y, Schilling J-G (2013) The mean composition of ocean ridge basalts. Geochem Geophys Geosyst 14:489–518

Gale A, Langmuir CH, Dalton CA (2014) The global systematics of ocean ridge basalts and their origin. J Petrol 55(6):1051–1082. https://doi.org/10.1093/petrology/egu017
Hart SR (1984) A large-scale isotope anomaly in the Southern Hemisphere mantle. Nature 309:753–757
Hofmann AW (1988) Chemical differentiation of the Earth: the relationship between mantle, continental crust, and oceanic crust. Earth Planet Sci Lett 90(3):297–314
Hofmann AW, White WM (1982) Mantle plumes from ancient oceanic crust. Earth Planet Sci Lett 57(2):421–436
Iwamori H, Albaréde F, Nakamura H (2010) Global structure of mantle isotopic heterogeneity and its implications for mantle differentiation and convection. Earth Planet Sci Lett 299(3):339–351
Kelley KA, Plank T, Grove TL, Stolper EM, Newman S, Hauri E (2006) Mantle melting as a function of water content beneath back-arc basins. J Geophys Res Solid Earth 111(B9)
Klein EM, Langmuir CH (1987) Global correlations of ocean ridge basalt chemistry with axial depth and crustal thickness. J Geophys Res Solid Earth Planets 92:8089–8115
Langmuir CH, Klein EM, Plank T (1992) Petrological systematics of mid-ocean ridge basalts: constraints on melt generation beneath ocean ridges. In: Phipps Morgan J, Blackman DK, Sinton JM (eds) Mantle flow and melt generation at mid-ocean ridges, Monograph 71, American geophysical union. AGU, Washington, DC, pp 183–280
Langmuir, C.H., A. Bézos, S. Escrig, S.W. Parman, Chemical systematics and hydrous melting of the mantle in back-arc basins, in: Fisher CR, Christie DM, Lee SM, and Givens S, (Ed), Back-arc spreading systems: geological, biological, chemical, and physical interactions 166, AGU, Washington, DC, 2006, pp. 87-146
Lehnert K, Su Y, Langmuir CH, Sarbas B, Nohl U (2000) A global geochemical database structure for rocks. Geochem Geophys Geosyst 1(5)
Lissenberg CJ, MacLeod CJ, Howard KA, Godard M (2013) Pervasive reactive melt migration through fast-spreading lower oceanic crust (Hess Deep, equatorial Pacific Ocean). Earth Planet Sci Lett 361:436–447
Niu Y, O'Hara MJ (2008) Global correlations of ocean ridge basalt chemistry with axial depth: a new perspective. J Petrol 49:633–664
Niu Y, Regelous M, Wendt IJ, Batiza R, O'Hara MJ (2002) Geochemistry of near-EPR seamounts: importance of source vs. process and the origin of enriched mantle component. Earth Planet Sci Lett 199(3):327–345
Rubin KH, Sinton JM (2007) Inferences on mid-ocean ridge thermal and magmatic structure from MORB compositions. Earth Planet Sci Lett 260:257–276
Schilling J-G (1975) Azores mantle blob: rare earth evidence. Earth Planet Sci Lett 25:103–115
Schilling JG, Kingsley R, Devine J (1982) Galapagos hot spot-spreading center system. 1, Spatial petrological and geochemical variations (83°W-101°W). J Geophys Res 87:5593–5610
Shen Y, Forsyth D (1995) Geochemical constraints on initial and final depths of melting at ocean ridges. J Geophys Res 100:2211–2237
Sinton JM, Fryer P (1987) Mariana trough lavas from 18°N: implications for the origin of back-arc basin basalts. J Geophys Res 92(B12):12782–12802
Stolper E, Newman S (1994) The role of water in the petrogenesis of Mariana trough magmas. Earth Planet. Sci Lett. 121:293–325
Sun SS, McDonough WS (1989) Chemical and isotopic systematics of oceanic basalts: implications for mantle composition and processes. Geol Soc Lond, Spec Publ 42(1):313–345
Sun SS, Nesbitt RW, Sharaskin AY (1979) Geochemical characteristics of mid-ocean ridge basalts. Earth Planet Sci Lett 44(1):119–138
Taylor B, Martinez F (2003) Back-arc basin basalt systematics. Earth Planet Sci Lett 210(3):481–497
White WM, Klein EM (2014) 4.13 – Composition of the oceanic crust. In: Holland HD, Turekian KK (eds) Treatise on geochemistry, 2nd edn. Elsevier, Oxford, pp 457–496

Mineral Defects

Kurt Schwartz[1] and Maik Lang[2]
[1]GSI Helmholtz Center for Heavy Ion Research, Darmstadt, Germany
[2]Department of Nuclear Engineering, University of Tennessee, Knoxville, TN, USA

Definition

Crystal defects can be most simply defined as distortions of the periodic arrangement of atoms in a "perfect" crystalline lattice. Above absolute zero temperature, defects are present in all crystals at certain concentrations. An increase in temperature increases the number of defects significantly. Depending on their dimensions, defects can be classified into point defects, line defects, planar defects, and bulk defects. Defects can be introduced in minerals through various means, such as self-radiation. Radiation-induced defects in minerals have been observed long before the discovery of radioactivity. Berzelius observed thermo-luminescence in gadolinite ($(Y,Ce)_2Fe^{2+}Be_2O_2(SiO_4)_2$) caused by α-decay of uranium and thorium trace elements (Berzelius 1815). Unaware of the underlying processes, Baumhauer etched fission-fragment tracks in apatite as early as the nineteenth century (Baumhauer 1894).

Classification of Defects

1. *Point (zero-dimensional) defects*

Point defects are distortions at a single lattice position, such as vacant atomic sites, which are called vacancies (Itoh and Stoneham 2001; Kittel 2004). Due to electrical charge neutrality, an equal number of anion and cation vacancies must be present at any time in ionic crystals (*Schotky defects*). *Frenkel defects* are a type of vacancy – interstitial pairs in the lattice, which can form if an atom is moved from its lattice site into an interstitial position. In ionic crystals both anion and cation Frenkel defects exist. Point defects can also be impurity elements substituting regular atoms (anions or cations in ionic crystals). Such defects can be introduced by contamination of minerals with foreign species. If the equilibrium charge of the impurity atom is different from the host crystal, vacancies can compensate the charge difference, e.g., Mg^{2+} impurity in NaCl (rock salt) has the microstructure of $Mg^{2+}v_c^-$ (v_c^- is a cation vacancy having a negative charge). The large variety of point defects that can be present in a mineral are illustrated in Fig. 1 for NaCl. Point defects are also color centers in dielectric materials which give rise to color in some minerals.